GDCh

Communications

Angewandte
Chemie
International Edition
www.angewandte.org

Photocatalysis | **Hot Paper**

Dye-Sensitized Photocatalysis: Hydrogen Evolution and Alcohol-to-Aldehyde Oxidation without Sacrifical Electron Donor

Deborah Romito, Chinju Govind, Vasilis Nikolaou, Ricardo J. Fernández-Terán,
Aspasia Stoumpidi, Eleni Agapaki, Georgios Charalambidis, Stéphane Diring, Eric Vauthey,*
Athanassios G. Coutsolelos,* and Fabrice Odobel*

Abstract: There is a growing interest in developing dye-sensitized photocatalytic systems (DSPs) to produce molecular hydrogen (H$_2$) as alternative energy source. To improve the sustainability of this technology, we replaced the sacrificial electron donor (SED), typically an expensive and polluting chemical, with an alcohol oxidation catalyst. This study demonstrates the first dye-sensitized system using a diketopyrrolopyrrole dye covalently linked to 2,2,6,6-tetramethyl-1-piperidine-*N*-oxyl (TEMPO) based catalyst for simultaneous H$_2$ evolution and alcohol-to-aldehyde transformation operating in water with visible irradiation.

Green hydrogen (H$_2$) is a potential clean energy carrier, stimulating the development of cheap and sustainable processes to produce this fuel from water and sunlight. In this context, artificial photosynthesis is the key process to

[*] Dr. D. Romito, Dr. V. Nikolaou, Dr. S. Diring, Dr. F. Odobel
Nantes Université, CNRS, CEISAM, UMR 6230
F-44000 Nantes (France)
E-mail: fabrice.odobel@univ-nantes.fr

Dr. C. Govind, Dr. R. J. Fernández-Terán, Dr. E. Vauthey
Department of Physical Chemistry
University of Geneva
30 Quai Ernest-Ansermet, CH-1211 Geneva (Switzerland)
E-mail: eric.vauthey@unige.ch

A. Stoumpidi, E. Agapaki, Prof. Dr. A. G. Coutsolelos
Laboratory of Bioinorganic Chemistry, Department of Chemistry
University of Crete
Voutes Campus, 70013 Heraklion, Crete (Greece)

Dr. G. Charalambidis
Theoretical and Physical Chemistry Institute

National Hellenic Research Foundation, 48 Vassileos Constantinou
Avenue, 11635 Athens (Greece)

Prof. Dr. A. G. Coutsolelos
Institute of Electronic Structure and Laser (IESL), Foundation for
Research and Technology – Hellas (FORTH), Vassilika Vouton, GR
70013 Heraklion, Crete (Greece)
E-mail: acoutsol@uoc.gr

produce energy-rich chemical fuels from abundant feedstocks.[1] Typical dye-sensitized photocatalytic systems (DSPs) are composed of a dye and a hydrogen evolution catalyst (HEC) co-grafted onto n-type semiconductor (n-SC) nanoparticles (NPs), such as titanium dioxide (TiO$_2$). These systems operate in the presence of an external sacrificial electron donor (SED) to ensure the rapid regeneration of the oxidized dye (PS$^+$).[2] However, employing SEDs (typically ascorbic acid AA or triethanolamine TEOA) represents a serious obstacle for both upscaling and commercialization, since they are expensive and polluting chemicals. To improve the sustainability and applicability of DSPs, the dye regeneration could be envisaged by exploiting an oxidation reaction, which would convert abundant substrates into value-added products instead of consuming a SED. Indeed, this strategy has been thoroughly explored by coupling proton reduction with water oxidation in a photo-electrochemical cell (PEC).[3] During this process O$_2$ is generally produced at the anode; however, oxygen has low economic value, and water oxidation is a kinetically and thermodynamically demanding reaction, which involves four electrons and requires high potential (1.23 V *vs.* Normal Hydrogen Electrode (NHE)).[4] On the other hand, the oxidation of alcohols into their corresponding aldehydes constitutes a promising alternative, as it is significantly less kinetically challenging (involves two electrons), it has a lower redox potential (−0.14 V vs. NHE for benzyl alcohol),[4] and it generates higher-value products.[5] Specifically, alcohols are abundant feedstock extracted from biomass, and their corresponding carbonyl derivatives are often used as valuable synthetic precursors in both chemical and pharmaceutical industries. Using alcohol oxidation to regenerate PS$^+$ was recently reported with the 2,2,6,6-tetramethyl-1-piperidine-*N*-oxyl (TEMPO) catalyst in dye-sensitized photoelectrocatalytic cells (DSPECs).[6] However, DSP is an attractive photocatalytic system owing to its simplicity in terms of preparation compared to DSPEC, which requires electrodes preparation, their wiring and a membrane to separate anolyte and catholyte. Moreover, there is only a handful of studies in DSPs employing alcohols as hole scavengers, but they are limited to methanol, ethanol and glycerol, and the efficiency and selectivity towards the carbonyl derivatives were not mentioned.[7] Interestingly, there are recent publications from Choi and co-workers[8] and Reisner and co-workers,[6e] respectively, dealing with coupling photocatalytic H$_2$ evolu-

tion or carbon dioxide (CO_2) reduction to selective alcohol oxidation processes, but these were only reported in PEC.

Herein, we report on an innovative DSP system for simultaneous H_2 evolution and selective benzyl alcohol oxidation working in water, without any sacrificial reagent. To accomplish this, we implemented a "photosensitizer-TEMPO" dyad (PS-TEMPO) instead of a PS, directing the regeneration of the dyad via alcohol-to-aldehyde oxidation. In addition, this photocatalytic system generates two easily separable products, namely H_2 which is released in the headspace of the reaction vessel, and aldehyde in solution which can be easily extracted (Figure 1). In this study, the dyad "PS-TEMPO" consists of a diketopyrrolopyrrole (DPP) photosensitizer covalently linked to a TEMPO catalyst (**DPP-TEMPO**, Scheme 1). DPP was selected as PS d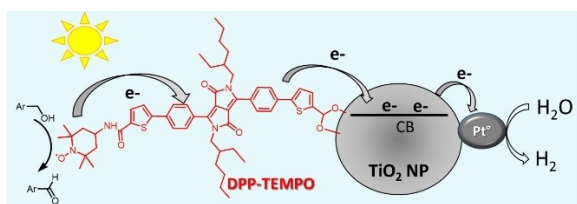ue to its high performance in dye-sensitized solar cells (DSSCs)[9] and DSPs.[10] A DPP bearing a neopentyl amide group was also prepared (**DPPref**, Scheme 1) to explore the impact of the TEMPO moiety. Furthermore, this allowed us to compare two different DSP approaches, namely, **DPP-TEMPO** (with covalently connected PS and catalyst) versus **DPPref** + **TEMPOsyl** (co-adsorbed on TiO_2).

The synthetic route for preparing **DPP-TEMPO** and **DPPref** is illustrated in Scheme S1. All molecules were characterized by ^1H and ^{13}C NMR spectroscopy and high-resolution mass spectrometry (Figures S1–S9, see ESI for details). In the absorption spectrum of both **DPP-TEMPO** and **DPPref**, the typical π–π* transition of DPP, centered around 490 nm, can be observed (Figure 2 and Table 1). Both compounds are fluorescent but, interestingly, the emission intensity and lifetime of **DPP-TEMPO** are not reduced relative to those of **DPPref**, indicating that neither photoinduced energy nor charge transfer towards TEMPO take place to a significant extent in the dyad (Figures 2 and S19). The electrochemical properties of **DPP-TEMPO** and **DPPref** were investigated by cyclic voltammetry in CH_2Cl_2 (Table 1). The driving force of the electron injection in TiO_2 from DPP* (ΔG_{inj}), and the hole shift from oxidized DPP to TEMPO (ΔG_{reg}) indicate that all these processes are thermodynamically allowed, with $\Delta G_{inj} \approx -0.2$ eV and $\Delta G_{reg} = -0.42$ eV, respectively (Table 1).

The DSP system was then prepared by functionalizing commercially available TiO_2 NPs with Pt^0 as HEC, and **DPP-TEMPO** as PS (see Electronic Supporting Information: ESI). Chemical binding of the dye to the TiO_2 surface via carboxylic acid was confirmed by infrared spectroscopic measurements showing the disappearance of the ν(C=O) stretching band of the free carboxylic moiety (1708 cm^{-1}) and the appearance of the new asymmetric stretching band of the O–C=O group (1638 cm^{-1}) when the dye is bound to TiO_2 (Figure S10), in agreement with a bidentate binding mode.[12]

The optimal photocatalytic conditions were determined by using *p*-methoxybenzyl alcohol (MeOBenzOH) as substrate for the oxidation, as well as by screening different pH values of a borate buffer, various **DPP-TEMPO** loadings, and the effect of different concentrations of Pt^0 on TiO_2 NPs (see ESI for details). The best catalytic performance was observed at pH = 8, with 24 nmol of **DPP-TEMPO** per mg of TiO_2 and with 3.2 nmol of Pt^0/mg of TiO_2 (Figures 3, S11–S14, Tables 2, S1–S3). As expected, all three components of the photocatalytic system are necessary for the reaction to occur, since neither H_2 production nor aldehyde conversion

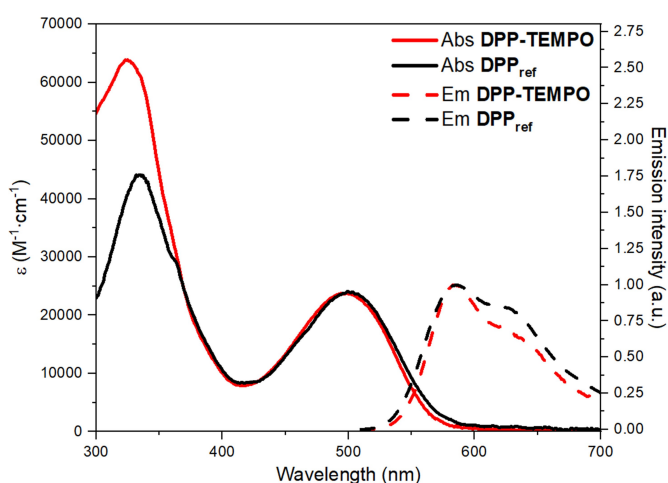**Figure 1.** Schematic representation of the dual-functional photocatalytic system investigated in this work.

Figure 2. Absorption (solid lines) and emission (dashed lines) spectra of solutions of **DPP-TEMPO** (in red) and **DPPref** (in black) in CH_2Cl_2 at r.t. $\lambda_{excit} = 490$ nm for fluorescence spectrum.

Table 1: Physico-chemical properties of **DPPref** and **DPP-TEMPO** recorded in CH_2Cl_2. All the potentials are referenced *vs.* saturated calomel electrode (SCE).

Dye	$\lambda_{abs}/\varepsilon$ (nm/M^{-1}·cm^{-1})	λ_{abs}/E_{00}[a] (nm/eV)	E_{Ox}(TEMPO$^+$/TEMPO) (V vs. SCE)	[b]E_{Ox}(DPP$^+$/DPP) (V vs. SCE)	[c]ΔG_{inj} (eV)	[d]ΔG_{reg} (eV)
DPPref	501/2.41·10^4	588/2.25	–	+1.21	−0.17	–
DPP-TEMPO	500/2.23·10^4	582/2.24	+0.75	+1.17	−0.20	−0.42

[a]Singlet excited state energy level (E_{00}) calculated with the wavelength at the intersection of normalized absorption and emission spectra; [b]irreversible process, here $E_{Ox} = E_a$; [c]calculated according to $\Delta G_{inj} = E_{Ox}(DPP^+/DPP) − E_{00} − E_{CB}(TiO_2)$ measured at pH = 8 with $E_{CB}(TiO_2) = −0.4 − 0.059 \cdot pH$;[11] [d]calculated according to $\Delta G_{reg} = E_{Ox}(TEMPO^+/TEMPO) − E_{Ox}(DPP^+/DPP)$.

DPP-TEMPO   **DPP$_{ref}$**   **TEMPO$_{syl}$**
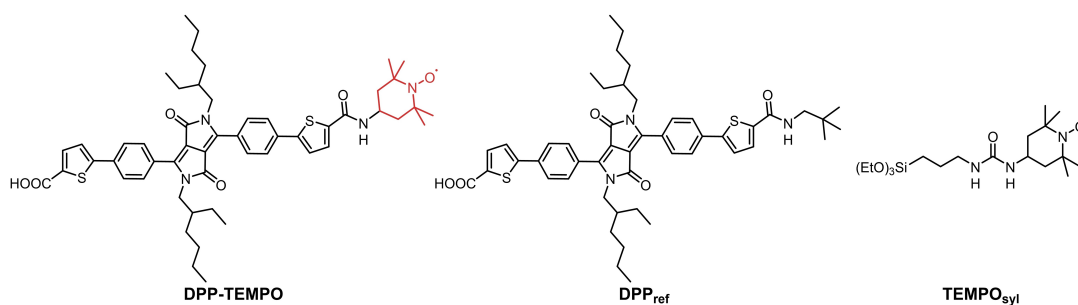
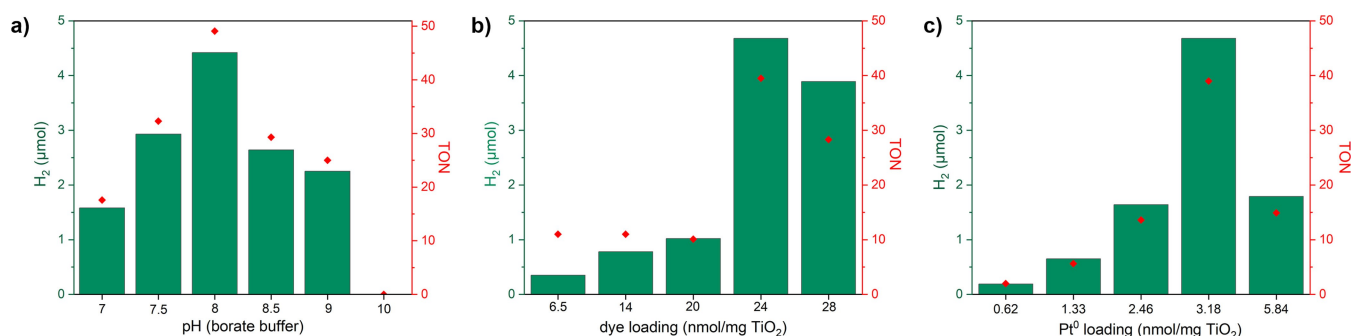**Scheme 1.** Molecular structures of the compounds used in this study.

Figure 3. Photocatalytic measurements displaying H$_2$ production (in green) and TON (in red) obtained using **DPP-TEMPO**/TiO$_2$/Pt^0 NPs a) screening the buffer borate at different pH, as well as varying b) the dye loading and c) the Pt^0 coverage.

Table 2: Photocatalytic results of the DSP systems recorded under different conditions.[a]

| Entry | Dye (nmol per mg of TiO$_2$)/TiO$_2$/Pt^0 | Alcohol | H$_2$ | | Aldehyde | |
			μmol	TON	conc. (mM)	μmol
1	**DPP-TEMPO**(18)/TiO$_2$/Pt^0	MeOBenzOH	4.2±0.2	47±2	0.59±0.09	2.9±0.02
2	**DPP-TEMPO**(24)/TiO$_2$/Pt^0	MeOBenzOH	4.7±0.3	39±4	0.74±0.09	3.7±0.1
3	**DPP-TEMPO**(24)/TiO$_2$/Pt^0	BenzOH	2.5±0.3	21±2	0.27±0.03	1.4±0.01
4	**DPP-TEMPO**(24)/TiO$_2$/Pt^0	CF$_3$BenzOH	3.4±0.2	28±2	0.42±0.06	2.1±0.02
5	**DPP$_{ref}$**(24)/TiO$_2$/Pt^0	MeOBenzOH	ND[b]	ND[b]	0.0025	0.012
6	TiO$_2$/Pt^0	MeOBenzOH	ND[b]	ND[b]	0.0015	0.0075
7	**DPP-TEMPO**(24)/TiO$_2$/Pt^0	–	ND[b]	ND[b]	–	–
8	**DPP$_{ref}$**(24)/TiO$_2$/Pt^0	–[c]	3.5±0.1	29±2	–	–
9	**DPP-TEMPO**(18)/TiO$_2$/Pt^0	–[c]	8.8±0.6	98±8	–	–
10	**DPP$_{ref}$**(19)/**TEMPO$_{syl}$**/TiO$_2$/Pt^0	MeOBenzOH	1.0±0.1	11±1	0.19±0.02	0.95±0.01

[a]The following standard conditions were employed: 5 mL of 0.1 M aqueous borate buffer at pH 8 + 10 mg of functionalized TiO$_2$ NPs/Pt^0(3.2 nmol); irradiation source: Green LED (525 nm, 10 mW/cm^2); irradiation time: 4 hours; amount of alcohol used: 50 mM. [b]Not detected; [c]0.1 M aqueous TEOA at pH 8 was used to replace the alcohol.

are observed when one component is missing (Tables 2 and S4). Similarly, the reaction does not proceed without light irradiation, confirming that the redox reactions are actually photodriven processes. At last, the replacement of **DPP-TEMPO** by the simple **DPP$_{ref}$** lacking TEMPO oxidation catalyst no longer promotes H$_2$ evolution nor alcohol oxidation.

The larger amount of H$_2$ relative to the photogenerated aldehyde is intriguing. Since these two products come from a two-electron redox reaction, we could expect a 1/1 ratio. This discrepancy could be most likely due to the lower intrinsic catalytic efficiency of TEMPO compared to that of Pt^0. Indeed, as Pt^0 is the most active HEC, it is not

unexpected that its efficiency is higher than that of TEMPO (see a more detailed discussion in ESI). Corroborating this assumption, a recent study by Reisner and co-workers also reported an unequal production of reduced and oxidized products by immobilizing a formate dehydrogenase onto TiO$_2$.[13]

As illustrated in Figure S17, H$_2$ evolution is interrupted after about 4 h of irradiation. To unveil the reason of the photocatalytic deactivation, **DPP-TEMPO** was desorbed from the functionalized TiO$_2$ NPs after photocatalysis with and without irradiation (see Figures S15–S16). The interruption of H$_2$ evolution is mainly attributed to: i) the photo-decomposition of the DPP photosensitizer (Figure S15)

rather than to ii) its detachment from the TiO$_2$ surface (Figures S12 and S16), although the instability of CO$_2$H anchoring group in aqueous media, and particularly in basic conditions, is well-known.[14]

Overall, these experiments demonstrate that a DSP sensitized with **DPP-TEMPO** produces H$_2$ with concomitant and selective alcohol oxidation into aldehyde without any SED, reaching 50 turnover number (TON). The rate of H$_2$ evolution calculated during the first 3 hours of the experiment is about 200 µmol·h^{-1}·g^{-1} of TiO$_2$; a value comparable to some previously published DSPs with SEDs.[2b] Having established the optimized conditions for photocatalytic methoxy-benzyl alcohol oxidation, the scope of the substrates was expanded by testing benzyl alcohol (BenzOH) and *p*-trifluoromethyl-benzyl alcohol (CF$_3$BenzOH), two additional substrates with different reactivity. Interestingly, although CF$_3$BenzOH displays the highest oxidation potential, a larger quantity of H$_2$ than with BenzOH was produced (Tables 2 and S7; Figure S17). This is most likely due to the hydrophobic nature of CF$_3$BenzOH, which would favour a closer contact within the layer of **DPP-TEMPO** on TiO$_2$ NPs. Noteworthy, an analogous trend was already reported in DSPECs with a zinc porphyrin-TEMPO sensitizer.[6c] To prove that the given photocatalytic system indeed works under sunlight, an additional photocatalytic measurement was performed using a sunlight simulator (AM 1.5 [1000 W/m^2], (Table S5). This results in a slightly lower H$_2$ production (3.3 µmol) and a lower TON (27), but confirms that this DSP works in real world sunlight conditions as well.

Aiming at comparing our novel approach with the classical one (using SED), photocatalytic experiments were carried out in the presence of TEOA (0.1 M, at pH = 8) as sacrificial electron donor. Remarkably, when **DPP$_{ref}$** is used as sensitizer, the generated H$_2$ is about 30 % less compared to the respective H$_2$ evolution using **DPP-TEMPO** (in presence of MeOBenzOH), showing that **DPP-TEMPO** with alcohol oxidation outperforms **DPP$_{ref}$** with SED (Table S8, Figure S18). Secondly, it is worth noting that **DPP-TEMPO** with TEOA as SED produces twice the amount of H$_2$ than **DPP$_{ref}$** under the same conditions. This is most likely due to the longer-lived charge-separated state of **DPP-TEMPO** compared to that of **DPP$_{ref}$** (see transient absorption spectroscopy study below).

Previous works on DSPEC for alcohol oxidation reported that significant catalytic activities could be measured when the catalyst was simply co-grafted along with the sensitizer on the TiO$_2$ surface.[6d,e] Testing the **DPP$_{ref}$**/**TEMPO$_{syl}$**/TiO$_2$/Pt^0 NPs in DSP conditions analogous to those employed with **DPP-TEMPO**, resulted in decreased photocatalytic efficiency, since both the amount of produced H$_2$ and aldehyde were reduced by over a factor four (~1 vs. 4.7 µmol(H$_2$), Table S9). Most likely, the weaker electronic communication between **TEMPO$_{syl}$** and **DPP$_{ref}$**, compared to that in **DPP-TEMPO**, diminishes the regeneration rate of the oxidized PS, accelerating charge recombination and degradation due to the instability of the DPP radical cation. In line with this interpretation, the exposition of the **DPP$_{ref}$**/**TEMPO$_{syl}$**/TiO$_2$/Pt^0 NPs to ambient light induces a fast bleaching within less than few hours in contrast with **DPP-**

TEMPO/TiO$_2$/Pt^0 NPs, which remains colored for much longer time in the same conditions.

In another photocatalytic experiment, we have investigated the performances of a DSP in which the catalyst, in the form 4-trimethylammonium-TEMPO (10 mM), is solubilized into the borate buffer in presence of **DPP$_{ref}$**-functionalized TiO$_2$ NPs (Table S6). In these conditions, the photocatalytic performances are much lower than those achieved with the **DPP-TEMPO**, underscoring thus the advantage of the covalent dyad.

Occurrence of charge injection from **DPP-TEMPO** into TiO$_2$ is confirmed by transient absorption (TA) measurements, which show the formation of the DPP cation (DPP$^+$) and an electron in the conduction band of TiO$_2$ in the visible (Figure 4)[15] and mid IR (Figures S20–S21) regions.[16] Subsequently, these features decay on several timescales ranging from a few ns to a few µs. The same measurements with **DPP$_{ref}$** films reveal that the decay dynamics of the DPP$^+$ band are essentially the same up to 20 ns, during which around 70 % of the initial intensity is lost (Figures S22–26). However, the remaining intensity decays with 50 ns and 1.4 µs time constants with **DPP-TEMPO** vs. 180 ns and 3.8 µs with **DPP$_{ref}$**. Similar differences are visible in the ground-state bleach region. These differences can be attributed to a hole shift from DPP$^{·+}$ to the TEMPO subunit occurring on the hundred ns timescale, which results in the neutralization of DPP$^{·+}$ and the repopulation of the electronic ground-state of the DPP subunit. The rest of the photocatalytic cycle cannot be investigated by TA since the hydroxylamine, nitroxide and oxoammonium forms of TEMPO have no spectroscopic signature in the 300–800 nm range. However, we can safely postulate that the oxoammonium can be reduced by alcohol to form the hydroxylamine and aldehyde with the release of two protons, as demonstrated in previous works.[4,6,17] Overall, hydroxylamine is
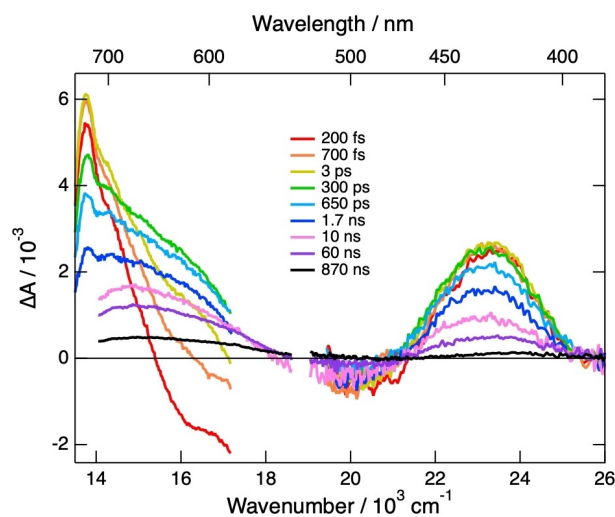

Figure 4. Transient absorption spectra recorded at various time delays after 532 nm excitation of a **DPP-TEMPO**/TiO$_2$ film in borate buffer (pH 8) illustrating the decay of the locally excited state (720 and 430 nm) and build-up and decay of the DPP radical cation (680 and 430 nm), due to charge injection and recombination.

oxidized into nitroxide, and then to oxoammonium by two consecutive holes coming from DPP$^+$. The holes can probably be supplied by the neighbouring PS$^+$ around the dyad owing to the known lateral hole migration within dye layer on TiO$_2$.[18]

In conclusion, we report for the first time on a dual-functional photocatalytic system based on TiO$_2$ nanoparticles sensitized by **DPP-TEMPO**, which simultaneously produces H$_2$ and oxidizes alcohols to aldehydes in water upon visible light irradiation. This is in sharp contrast to the traditional approach of DSPs, which requires SEDs for regenerating the oxidized dye; thus, rendering DSPs for H$_2$ evolution more compatible towards future practical applications. In addition, TEMPO can catalyze other useful oxidation reactions, i.e. preparation of imines, nitriles, and unsaturated heterocycles.[17] Consequently, the scope of the substrates can certainly be expanded following a similar strategy. Importantly, this study gives a new impetus to DSP by showing that a two-hole oxidation process, such as alcohol oxidation, is a viable reaction to couple with a reduction reaction targeting the elimination of the SED and the generation of two added-value chemicals. Moreover, other reduction catalysts besides HECs could be implemented in the above described DSPs, such as those for CO$_2$ and N$_2$ reduction. Finally, our study shows that better performing DSPs could be engineered if a secondary electron donor is linked to the dye to prolong the final charge-separated state lifetime (e$^-$/TiO$_2$-DPP$^+$ vs. e$^-$/TiO$_2$-TEMPO-DPP$^+$). This work opens new horizons for developing DSPs without SEDs, based on the association of a dye and a TEMPO catalyst for oxidizing organic compounds. Current enhancements of the present system are ongoing in our research group and include the application of more electrochemically stable dyes than DPP, bearing stronger binding groups than the carboxylic acid.

Supporting Information

The authors have cited additional references within the Supporting Information.[19–27]

Conflict of Interest

The authors declare no conflict of interest.

Data Availability Statement

The data that support the findings of this study are available in the supplementary material of this article.

[1] a) M. E. El-Khouly, E. El-Mohsnawy, S. Fukuzumi, *J. Photochem. Photobiol. C* **2017**, *31*, 36–83; b) B. Zhang, L. Sun, *Chem. Soc. Rev.* **2019**, *48*, 2216–2264.

[2] a) G. Reginato, L. Zani, M. Calamante, A. Mordini, A. Dessì, *Eur. J. Inorg. Chem.* **2020**, *2020*, 899–917; b) J. F. Huang, Y. Lei, T. Luo, J. M. Liu, *ChemSusChem* **2020**, *13*, 5863–5895; c) J. Willkomm, K. L. Orchard, A. Reynal, E. Pastor, J. R. Durrant, E. Reisner, *Chem. Soc. Rev.* **2016**, *45*, 9–23.

[3] S. Bae, J. E. Jang, H. W. Lee, J. Ryu, *Eur. J. Inorg. Chem.* **2019**, *2019*, 2040–2057.

[4] F. Wang, S. S. Stahl, *Acc. Chem. Res.* **2020**, *53*, 561–574.

[5] a) H. Sterckx, B. Morel, B. U. Maes, *Angew. Chem. Int. Ed.* **2019**, *58*, 7946–7970; b) C. R. Lhermitte, K. Sivula, *ACS Catal.* **2019**, *9*, 2007–2017; c) Y. Xu, B. Zhang, *ChemElectroChem* **2019**, *6*, 3214–3226.

[6] a) D. F. Bruggeman, T. M. Bakker, S. Mathew, J. N. Reek, *Chem. Eur. J.* **2021**, *27*, 218–221; b) S. Li, S. Kim, A. H. Davis, J. Zhuang, E. W. Shuler, D. Willinger, J.-J. Lee, W. Zheng, B. D. Sherman, C. G. Yoo, *ACS Catal.* **2021**, *11*, 3771–3781; c) E. Nikoloudakis, P. B. Pati, G. Charalambidis, D. S. Budkina, S. Diring, A. Planchat, D. Jacquemin, E. Vauthey, A. G. Coutsolelos, F. Odobel, *ACS Catal.* **2021**, *11*, 12075–12086; d) D. Bruggeman, S. Mathew, R. Detz, J. Reek, *Sustain. Energy Fuels* **2021**, *5*, 5707–5716; e) D. Antón-García, E. Edwardes Moore, M. A. Bajada, A. Eisenschmidt, A. R. Oliveira, I. A. Pereira, J. Warnan, E. Reisner, *Nat. Synth.* **2022**, *1*, 77–86; f) D. F. Bruggeman, A. A. Laporte, R. J. Detz, S. Mathew, J. N. Reek, *Angew. Chem. Int. Ed.* **2022**, *61*, e202200175.

[7] L. Zani, M. Melchionna, T. Montini, P. Fornasiero, *J. Phys. Energy* **2021**, *3*, 031001.

[8] H. G. Cha, K.-S. Choi, *Nat. Chem.* **2015**, *7*, 328.

[9] a) J. Warnan, L. Favereau, Y. Pellegrin, E. Blart, D. Jacquemin, F. Odobel, *J. Photochem. Photobiol. A* **2011**, *226*, 9–15; b) L. Favereau, J. Warnan, Y. Pellegrin, E. Blart, M. Boujtita, D. Jacquemin, F. Odobel, *Chem. Commun.* **2013**, *49*, 8018–8020; c) T. W. Holcombe, J.-H. Yum, Y. Kim, K. Rakstys, M. Grätzel, *J. Mater. Chem. A* **2013**, *1*, 13978–13983; d) F. Zhang, K.-J. Jiang, J.-H. Huang, C.-C. Yu, S.-G. Li, M.-G. Chen, L.-M. Yang, Y.-L. Song, *J. Mater. Chem. A* **2013**, *1*, 4858–4863.

[10] J. Warnan, J. Willkomm, J. N. Ng, R. Godin, S. Prantl, J. R. Durrant, E. Reisner, *Chem. Sci.* **2017**, *8*, 3070–3079.

[11] L. Kavan, N. Tétreault, T. Moehl, M. Grätzel, *J. Phys. Chem. C* **2014**, *118*, 16408–16418.

[12] K. S. Finnie, J. R. Bartlett, J. L. Woolfrey, *Langmuir* **1998**, *14*, 2744–2749.

[13] E. Lam, M. Miller, S. Linley, R. R. Manuel, I. A. Pereira, E. Reisner, *Angew. Chem. Int. Ed.* **2023**, *62*, e202215894.

[14] a) L. Zhang, J. M. Cole, *ACS Appl. Mater. Interfaces* **2015**, *7*, 3427–3455; b) K. L. Materna, R. H. Crabtree, G. W. Brudvig, *Chem. Soc. Rev.* **2017**, *46*, 6099–6110.

[15] A. Yamakata, T.-a. Ishibashi, H. Onishi, *Chem. Phys. Lett.* **2001**, *333*, 271–277.

[16] F. Lakadamyali, A. Reynal, M. Kato, J. R. Durrant, E. Reisner, *Chem. Eur. J.* **2012**, *18*, 15464–15475.

[17] J. E. Nutting, M. Rafiee, S. S. Stahl, *Chem. Rev.* **2018**, *118*, 4834–4885.

[18] a) K. Hu, G. J. Meyer, *Langmuir* **2015**, *31*, 11164–11178; b) H.-Y. Chen, S. Ardo, *Nat. Chem.* **2018**, *10*, 17–23.

[19] J. S. Beckwith, A. Aster, E. Vauthey, *Phys. Chem. Chem. Phys.* **2022**, *24*, 568–577.

[20] B. Lang, S. Mosquera-Vázquez, D. Lovy, P. Sherin, V. Markovic, E. Vauthey, *Rev. Sci. Instrum.* **2013**, *84*, 073107.

[21] M. Koch, R. Letrun, E. Vauthey, *J. Am. Chem. Soc.* **2014**, *136*, 4066–4074.

[22] D. Cao, Q. Liu, W. Zeng, S. Han, J. Peng, S. Liu, *Macromolecules* **2006**, *39*, 8347–8355.

[23] P. Brogdon, L. E. McNamara, A. Peddapuram, N. I. Hammer, J. H. Delcamp, *Synth. Met.* **2016**, *222*, 66–75.

[24] L. Zhang, J. M. Cole, *J. Mater. Chem. A* **2017**, *5*, 19541–19559.

[25] J. Humphreys, F. Pop, P. A. Hume, A. S. Murphy, W. Lewis, E. S. Davies, S. P. Argent, D. B. Amabilino, *CrystEngComm* **2021**, *23*, 1796–1814.

[26] S. Nishioka, K. Hojo, D. Saito, I. Yamamoto, T. E. Mallouk, K. Maeda, *Appl. Catal. A* **2023**, *654*, 119086.

[27] P. E. Hartnett, S. M. Dyar, E. A. Margulies, L. E. Shoer, A. W. Cook, S. W. Eaton, T. J. Marks, M. R. Wasielewski, *Chem. Sci.* **2015**, *6*, 402–411.